



Cytotoxicity activity and *in silico* studies from ethanol, ethyl acetate, and n-hexane extracts of *Marchantia paleacea* liverwort herb on MCF-7 and T47D breast cancer cells

Dicki Bakhtiar Purkon^{1,2*}, Irvan Herdiana¹, Mimin Kusmiyati¹, Eva Dania Kosasih^{3,4}, Nur Aji⁴, Faizah Min Fadhlillah⁵, Muhamad Iqbal Ramadhianto^{6,7}, Jihan Amirah Salsabila¹, Putri Dwi Handayani¹

¹Department of Pharmacy, Poltekkes Kemenkes Bandung, Bandung City, West Java, 40161, Indonesia

²Center of Excellence on Utilization of Local Material for Health Improvement, Poltekkes Kemenkes Bandung, Bandung City, West Java, 40171, Indonesia

³Department of Pharmacy, Universitas Soedirman, Central Java, Indonesia

⁴Department of Pharmacy, Poltekkes Kemenkes Tasikmalaya, Tasikmalaya City, West Java, 46115, Indonesia

⁵Department of Pharmacy, Faculty of Mathematics and Natural Sciences, Universitas Garut, Garut Regency, West Java, 4451, Indonesia

⁶Department of Pharmacy, Universitas Muhammadiyah Bandung, West Java, Indonesia

⁷Magister of Pharmacy, Pharmaceutical Chemistry Science, Institut Teknologi Bandung, West Java, Indonesia

ARTICLE INFO

Article Type:
Original Article

Article History:
Received: 7 May 2025
Revised: 26 Nov. 2025
Accepted: 26 Nov. 2025
published: 1 Jan. 2026

Keywords:
Bisbibenzyl compounds
Marchantia paleacea
Apoptosis
Breast neoplasms
Computational biology

ABSTRACT

Introduction: *Marchantia paleacea* contains macrocyclic bisbibenzyls, including marchantins with known cytotoxic, antioxidant, and antimicrobial activities, with no known mechanism of action. This study aimed to evaluate the cytotoxic potential of three solvent extracts—70% ethanol (EEMP), ethyl acetate (EAEMP), and n-hexane (NHEMP)—of *M. paleacea* and to assess molecular interactions of their bioactive compounds through *in silico* simulations against cancer-related proteins.

Methods: Cytotoxicity was determined on MCF-7 and T47D breast cancer cell lines using the MTT assay, with doxorubicin as a positive control. Chemical profiling of the most active extract was performed using Fourier-transform infrared (FTIR) spectroscopy and gas chromatography-mass spectrometry (GC-MS), followed by molecular docking against carbonic anhydrase II (CA-II, PDB ID: 1T47) and cyclin-dependent kinase 2 (CDK2, PDB ID: 1T46).

Results: Among the tested extracts, EAEMP showed the strongest cytotoxicity (IC₅₀ = 8.68 µg/mL for MCF-7; 12.78 µg/mL for T47D), compared with EEMP (119.2 and 64.33 µg/mL) and NHEMP (62.07 and 229.8 µg/mL). GC-MS identified Marchantin A, B, and C as major constituents, with Marchantin C exhibiting the highest docking affinity (ΔG = -8.62 kcal/mol) at residues D810 and E640.

Conclusion: The ethyl-acetate extract of *M. paleacea* demonstrates significant *in vitro* and *in silico* anticancer potential, suggesting its promise as a semi-polar source of cytotoxic bisbibenzyl compounds for future natural anticancer drug development.

Implication for health policy/practice/research/medical education:

The findings of this study highlight the potential of *Marchantia paleacea* as a source of semi-polar bioactive compounds, particularly bisbibenzyl derivatives, with significant cytotoxic activity against breast cancer cell lines. In clinical and research practice, the results encourage further preclinical evaluation, standardization of extraction methods, and exploration of structure-activity relationships to optimize therapeutic efficacy.

Please cite this paper as: Purkon DB, Herdiana I, Kusmiyati M, Kosasih ED, Aji N, Fadhlillah FM, et al. Cytotoxicity activity and *in silico* studies from ethanol, ethyl acetate, and n-hexane extracts of *Marchantia paleacea* liverwort herb on MCF-7 and T47D breast cancer cells. J Herbmed Pharmacol. 2026;15(1):36-50. doi: 10.34172/jhp.2026.53139.

Introduction

Breast cancer is one of the most common types of cancer in women worldwide and a major cause of morbidity and mortality. Although various therapies, such as chemotherapy, hormonal therapy, and immunotherapy, have been developed, significant side effects and drug resistance remain major challenges in breast cancer treatment. Breast cancer is also a type of cancer that causes death, with an average of 38 deaths per 100,000 women worldwide (1). Therefore, new, safer, and more effective therapeutic alternatives are needed, including the development of natural (herbal)-based anticancer agents.

Several types of plants in Indonesia are known to produce secondary metabolites with pharmacological activity, and their potential can be utilized as raw materials for the development of drugs, especially anticancer drugs. Many modern drugs used clinically are derived from medicinal plants. One potential plant for research and development is the liverwort herb *Marchantia paleacea*, which has been traditionally used in Latin America, China, and Indonesia. Some of the pharmacological properties that have been tested on the liverwort herb *M. paleacea* are antioxidant, vasorelaxant, antibiotic/antibacterial, immunostimulant, and hepatoprotective properties (2).

Several studies have reported that liverworts contain bioactive compounds, such as flavonoids, phenols, and bisbibenzyls (3). Compounds in the liverwort genus *Marchantia* have potential biological activities, including antimicrobial, anti-inflammatory, and anticancer properties (4). The compounds Marchantin A, B, and C, found in *M. paleacea* and previously identified in other species of the same genus, such as *Marchantia polymorpha*, have demonstrated cytotoxic activity in vitro against breast cancer cells (5). However, there is limited scientific data regarding the anticancer activity, particularly the anti-breast cancer activity, of the liverwort herb *Marchantia paleacea* in vitro (cytotoxic) on specific types of cancer cells.

In this study, we evaluated the cytotoxic activities of extracts prepared from 70% ethanol, ethyl acetate, and n-hexane in *M. paleacea* against MCF-7 and T47D breast cancer cell lines using the MTT assay. The extracts with the highest activity were further analyzed using Fourier-transform infrared (FTIR) spectroscopy and gas chromatography-mass spectrometry (GC-MS) to identify the bioactive compounds contributing to the anticancer activity. *In silico* studies were also conducted to evaluate the interactions of these bioactive compounds with cancer-related protein targets, providing a strong scientific basis for their further development as natural or herbal-based anticancer agents (6).

Materials and Methods

Materials

The primary materials used in this study were extracts

of *M. paleacea*, prepared at the Pharmacognosy-Phytochemistry and Pharmacology Laboratories, Department of Pharmacy, Poltekkes Kemenkes Bandung. The MCF-7 and T47D breast cancer cell lines, along with standard cell-culture reagents, were prepared at the Central Laboratory and Cell Culture-Cytogenetics Laboratory, Universitas Padjadjaran, Bandung, Indonesia. All cytotoxicity and phytochemical analyses were conducted using standard laboratory equipment, including a biosafety cabinet, CO₂ incubator, inverted microscope, ELISA reader, rotary vacuum evaporator, FTIR spectrometer, and GC-MS instrument.

Marchantia paleacea samples were collected from Kampung Padajaya Street, Sindangjaya Village, Cipanas District, Cianjur, West Java, Indonesia (6°44'35.4"S, 107°02'45.1"E), outside the Cibodas Botanical Garden area. Only mature, morphologically uniform thalli were selected, and all samples were collected during the same season to minimize variability. Species identification was confirmed at the Plant Taxonomy Laboratory, Department of Biology, FMIPA, Padjadjaran University (Herbarium document number: 30/HB/05/2023).

Preparation and determination of test plants, and the extraction process with three types of solvents (70% ethanol, ethyl acetate, and n-hexane)

Fresh *M. paleacea* herb (21.0610 kg) was air-dried to reduce moisture for storage. Extraction was performed by cold maceration using three solvents: 70% ethanol (polar), ethyl acetate (semi-polar), and n-hexane (non-polar), with periodic stirring, repeated three times for each solvent. The resulting liquid extracts were concentrated by rotary vacuum evaporation under the following conditions: 70% ethanol at 60 °C and 175 mbar, ethyl acetate at 40 °C and 240 mbar, and n-hexane at 40 °C and 360 mbar.

The resulting paste extracts were used for cytotoxicity, FTIR, and GC-MS analyses. The three solvents with different polarities enabled qualitative and quantitative assessments of secondary metabolites (e.g., flavonoids, terpenoids, and bisbibenzyls) with potential cytotoxic activity (7).

Anti-breast cancer activity of ethanol, ethyl acetate, and n-hexane extracts of *Marchantia paleacea* against MCF-7 and T47D breast cancer cell lines

MCF-7 and T47D cells were seeded in 96-well plates and cultured at 37 °C with 5% CO₂ until they reached 80% confluence. After treatment with the samples and 48 hours of incubation, MTT reagent was added, and the absorbance was measured using a Multiskan® ELISA reader (8). Complete RPMI medium (10% FBS and 1% penicillin/streptomycin) was used. Paste extracts of *M. paleacea* (70% ethanol, ethyl acetate, and n-hexane) were dissolved in DMSO to prepare 100,000 µg/mL stock solutions, which were serially diluted in RPMI to final

concentrations of 7.81–1000 µg/mL (9).

Cells with $\geq 80\%$ confluence were harvested using trypsin-EDTA, centrifuged at 1500 rpm for 5 minutes, and resuspended in complete medium. Cell numbers and viability were assessed by trypan blue exclusion using a hemocytometer. Cells were seeded in 96-well plates at 5,000 cells/well in 200 µL medium, then incubated at 37 °C with 5% CO₂ for 24 hours (or until 80% confluency) before treatment (9).

After labeling, the medium was removed from each well and replaced with 200 µL of the test sample at various concentrations or control medium. All treatments were performed in triplicate, and the plates were incubated for 48 hours (9). After treatment, the wells were rinsed with PBS, and 100 µL of MTT reagent was added. Plates were incubated at 37 °C with 5% CO₂ for 2–4 48 hours to allow formazan formation. After removing the reagent, DMSO was added to dissolve the formazan crystals. Absorbance was measured at 550 nm using a Multiskan EX® ELISA reader (8).

Analysis of FTIR and GC-MS of the extract types with the most optimal IC₅₀ values

FTIR analysis was conducted on the extract with the lowest IC₅₀ to identify the functional groups related to cytotoxic activity. Samples were prepared on KBr discs (1:10 ratio), and spectra were obtained using a Nicolet iS10 FTIR (4000–400 cm⁻¹). The major peaks (O–H, C=O, and C=C) were associated with bioactive compounds, such as flavonoids, phenols, and bisbibenzyls (10).

GC-MS analysis was performed on the extract with the lowest IC₅₀ to identify the major bioactive compounds. An RTX-5MS column (30 m × 0.25 mm, 0.25 µm) was used with helium as the carrier gas (1 mL/min), employing a temperature program from 60 °C (2 minutes) to 280 °C at a rate of 10 °C/min. The compounds were identified by comparison with the NIST/Wiley library, and the main peak was considered the primary compound. The relationship between the identified compounds and IC₅₀ was evaluated for pharmacological relevance (11).

In silico study of various secondary metabolite compounds in *Marchantia paleacea* as a breast cancer inhibitor

Preparation of test ligands

The active compound Marchantin C from *M. paleacea* was selected as the test ligand. The 2D and 3D structures were generated using ChemDraw, and geometric optimization was performed using Gaussian 09 with DFT/B3LYP and a 6-31G basis set (12).

Test target preparation

The protein targets (C-Kit tyrosine kinase, PDB ID: 1T46; carbonic anhydrase II, PDB ID: 1CNX; and protein kinase, PDB ID: 3POZ) were downloaded from the Protein Data Bank (PDB) (*.pdb format). The grid box parameters

were set based on the active site size (using CASTp), ligand size, and conformational flexibility: 1CNX (center: x=28.5, y=-14.3, z=5.6; size: 30×30×30 Å), 3POZ (center: x=-18.5, y=25.6, z=42.4; size: 40×40×40 Å) (13).

Docking validation

Docking validation was performed by redocking co-crystallized ligands (prepared in Discovery Studio) using AutoDock 4.2.6, with grid boxes centered on the corresponding ligands. The parameters included 100 GA runs; validation was accepted if the RMSD was ≤ 2 Å. All ligands fit within the grid and showed stable binding, confirming the adequacy of the grid (13).

Docking simulation

Molecular docking simulations were conducted using AutoDock 4.2.6 with validated grid box settings. The binding affinity (ΔG), inhibition constant (K_i), and ligand–target interactions were analyzed and visualized using Discovery Studio Visualizer 2016 (14). Grid box dimensions and justification of their suitability for accommodating all tested ligands, especially compounds 2 (Marchantin A), 3 (Marchantin B), and 4 (Marchantin C), were confirmed to be appropriate for molecular docking simulations.

Data analysis

Data were analyzed using Microsoft Excel 2024 and GraphPad Prism (version 10.4.1). Cytotoxicity (MTT assay) data for MCF-7 and T47D cells were evaluated using nonlinear regression (four-parameter logistic curve) to calculate IC₅₀ values and ANOVA to assess the significance of extract concentration on cell viability (15).

Results

Preparation and determination of test plants, and the extraction process with three types of solvents (70% ethanol, ethyl acetate, and n-hexane)

Fresh *M. paleacea* was collected from Sindangjaya Village, Cianjur, West Java (outside the Cibodas Botanical Garden area), totaling 21.061 kg. Plant identity was confirmed at the Plant Taxonomy Laboratory, FMIPA, Padjadjaran University (Herbarium No. 36/HB/05/2023). Simplicia yield was 11.52% (w/w) with a water content of 12.75 ± 0.05%.

Anti-breast cancer activity of the ethanol, ethyl acetate, and n-hexane extracts of *Marchantia paleacea* against MCF-7 and T47D breast cancer cells

Cytotoxicity assays on MCF-7 cells revealed varying efficacies among the extracts of *M. paleacea* prepared using 70% ethanol (EEMP), ethyl acetate (EAEMP), and n-hexane (NHEMP) (Figure 1). Figure 1 shows the relationship curve between the percentage of normalized absorbance (%) and log concentration from various

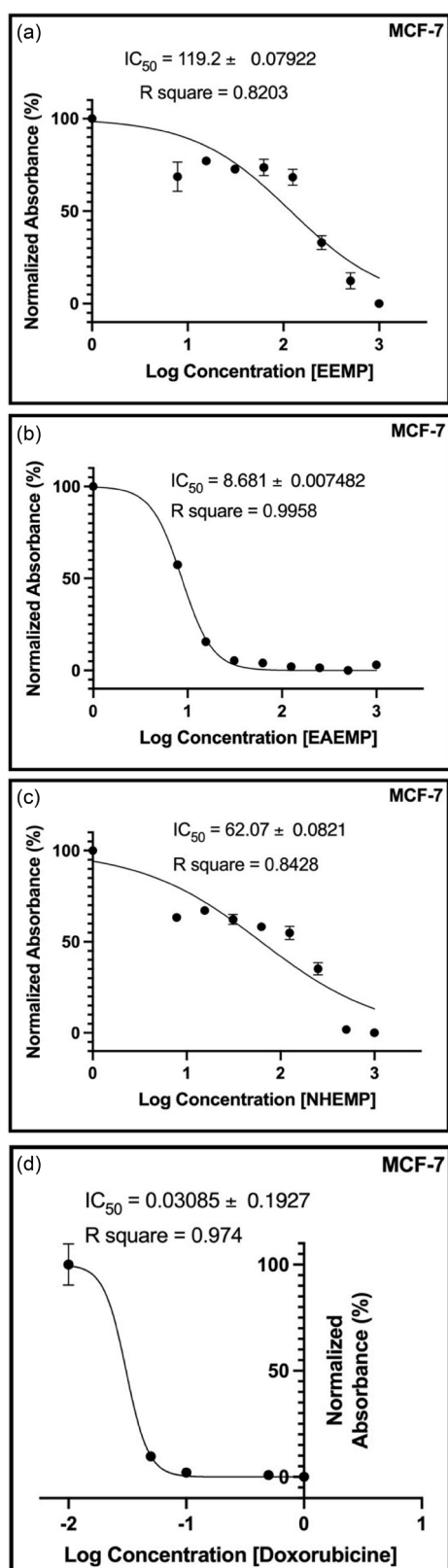


Figure 1. Dose-response curve of various extracts of *Marchantia paleacea* against MCF-7 breast cancer cells. The data curve shows the relationship between normalized absorbance (%) and log concentration used for IC_{50} determination after 48 hours of treatment. (a) 70% ethanol extract (EEMP), (b) ethyl-acetate extract (EAEMP), and (c) n-hexane extract (NHEMP) of *M. Paleacea*. (d) doxorubicin as a standard control. IC_{50} values were obtained using non-linear regression (four-parameter logistic model) in GraphPad Prism version 10.4.1. IC_{50} : half-maximal inhibitory concentration.

test preparations of *M. paleacea* liverwort herb extracts (EEMP, EAEMP, and NHEMP) and the positive control doxorubicin on MCF-7 breast cancer cells after 48 hours (T48). The cytotoxic test results showed a significant difference in the IC_{50} values between the three extracts and the positive control, reflecting the effectiveness of each test compound in inhibiting cancer cell growth. The ethyl acetate extract (EAEMP) exhibited the highest cytotoxic potential, with an IC_{50} value of $8.681 \pm 0.0075 \mu\text{g/mL}$ and a coefficient of determination (R^2) value of 0.9958. These results indicate that EAEMP is highly effective in inducing cancer cell death, especially in the MCF-7 cancer cell line. NHEMP and EEMP showed moderate activity against MCF-7 cells, with IC_{50} values of $62.07 \pm 0.08 \mu\text{g/mL}$ ($R^2 = 0.84$) and $119.2 \pm 0.08 \mu\text{g/mL}$ ($R^2 = 0.82$), respectively. Doxorubicin was markedly more potent ($IC_{50} = 0.03 \pm 0.19 \mu\text{g/mL}$, $R^2 = 0.97$), supporting its status as a standard anticancer reference.

Figure 2 presents the graphical relationship between normalized absorbance (%) and the logarithm of extract concentration, showing that the EAEMP extract produced the steepest slope and lowest IC_{50} value, indicating the strongest cytotoxic response. The other extracts, EEMP and NHEMP, showed progressively weaker activities, while doxorubicin served as the positive control with the highest potency. Table 1 summarizes the quantitative IC_{50} values and determination coefficients (R^2) obtained from these dose-response curves. The EAEMP exhibited the highest potency ($IC_{50} = 12.78 \pm 0.03 \mu\text{g/mL}$, $R^2 = 0.98$), followed by the ethanol extract ($IC_{50} = 64.33 \pm 0.02 \mu\text{g/mL}$, $R^2 = 0.98$), and the n-hexane extract ($IC_{50} = 229.8 \pm 0.06 \mu\text{g/mL}$, $R^2 = 0.87$). Doxorubicin, used as a reference anticancer agent, showed an $IC_{50} = 0.02 \pm 0.13 \mu\text{g/mL}$ ($R^2 = 0.85$). These results confirm that semi-polar extracts, particularly EAEMP, contain more bioactive phenolic and terpenoid constituents contributing to higher cytotoxic potential compared to polar or non-polar fractions.

FTIR and GC-MS test results of the ethyl acetate extract of *Marchantia paleacea* liverwort herb

Figure 3 and Table 2 show that the main FTIR peaks correspond to O-H (3389.8 cm^{-1}), aliphatic C-H (2922.7 , 2852.4 cm^{-1}), C=O (1711.6 cm^{-1}), aromatic C=C (1602.2 , 1583.8 cm^{-1}), C-O (1233.0 cm^{-1}), and aromatic ring deformations (694.8 , 721.5 cm^{-1}), indicating the presence of alcohols, phenols, carbonyl, and aromatic compounds. GC-MS analysis of the ethyl acetate extract (Figure 4, Table 3) revealed 33 unique compounds. The most abundant peak (RT = 51.57 minutes; area = 250,448; 36.5%) indicated a dominant bioactive component. Other major peaks were observed at 26.09, 38.99, and 43.57 minutes. These results, in conjunction with the FTIR findings, suggest the presence of diverse active compounds that likely contribute to the cytotoxic effects against MCF-7 and T47D cells. The Y-axis in Figure 4 represents total ion

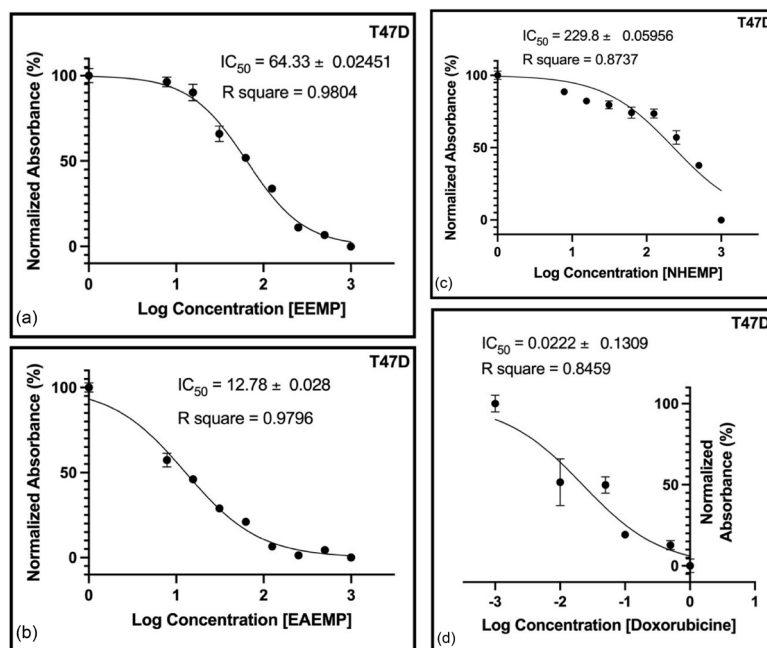


Figure 1. Dose–response curve of various extracts of *Marchantia paleacea* against MCF-7 breast cancer cells. The data curve shows the relationship between normalized absorbance (%) and log concentration used for IC_{50} determination after 48 hours of treatment. (a) 70% ethanol extract (EEMP), (b) ethyl-acetate extract (EAEMP), and (c) n-hexane extract (NHEMP) of *M. Paleacea*. (d) doxorubicin as a standard control. IC_{50} values were obtained using non-linear regression (four-parameter logistic model) in GraphPad Prism version 10.4.1. IC_{50} : half-maximal inhibitory concentration.

current (arbitrary units), reflecting the relative abundance of each detected compound.

The GC–MS analysis of the ethyl acetate extract of *M. paleacea* identified several bioactive compounds, including terpenoids (phytol, squalene), fatty acids (n-hexadecanoic acid, linoleic acid), sterols (β -sitosterol, stigmasterol), and bisbibenzyl derivatives (Marchantin A–C). Among these, Marchantin C showed a dominant peak (RT = 38.99 minutes, Area% = 9.97%), supporting its role as the major cytotoxic compound consistent with the *in silico* and *in vitro* results.

In silico study of various secondary metabolite compounds in the *Marchantia paleacea* liverwort herb as a breast cancer inhibitor

Lipinski rule of five

Table 4 shows that all *M. paleacea* compounds, as well

as reference Marchantins A–C, met Lipinski's rule of five, suggesting good oral drug-likeness. In contrast, the positive controls (doxorubicin, vinorelbine, vinblastine, and vincristine) did not meet these criteria, consistent with their use as intravenous drugs. Notably, L7 satisfied Lipinski's rule and was a potential oral drug candidate, while L9's high lipophilicity favors topical or injectable use. Lipinski's parameters (molecular weight, HBD, HBA, log P, and MR) were used to assess the oral drug suitability.

Geometry optimization

Compounds that fulfilled Lipinski's five rules were then subjected to geometry optimization to obtain the minimum conditions for compounds that can interact and bind maximally to the target.

Table 1. Results of anti-breast cancer activity ($IC_{50} \pm SEM$, $\mu g/mL$) of various extracts of *Marchantia paleacea* and doxorubicin on MCF-7 and T47D breast cancer cell lines after 48 hours incubation

No.	Sample	IC_{50} value	
		MCF-7 breast cancer cell line (ppm or $\mu g/mL$)	T47D breast cancer cell line (ppm or $\mu g/mL$)
1.	EEMP	119.20 \pm 0.0792	64.33 \pm 0.0245
2.	EAEMP	8.68 \pm 0.0075	12.78 \pm 0.0280
3.	NHEMP	62.07 \pm 0.0821	229.80 \pm 0.0596
4.	Doxorubicin	0.03 \pm 0.1927	0.02 \pm 0.1309

Statistical significance was determined using one-way ANOVA followed by Tukey's post-hoc test for multiple comparisons among all extracts and doxorubicin ($P < 0.05$). Values are expressed as mean \pm SEM ($n = 3$). EEMP, EAEMP, and NHEMP: Ethanol, ethyl-acetate, and n-hexane extracts of *M. paleacea*. EAEMP exhibited significantly higher cytotoxicity than both EEMP and NHEMP ($P < 0.05$). Meanwhile, there was a significant difference between EEMP and NHEMP on both MCF-7 and T47D cell lines ($P < 0.05$), indicating a polarity-dependent cytotoxic response.

Table 2. Fourier transform infra-red (FTIR) interpretation results of the ethyl acetate extract of the *Marchantia paleacea* liverwort

Peak position (cm ⁻¹)	Intensity	Functional group	Possible compounds
694.75	71.36	Out-of-plane deformation of aromatic rings (C-H)	Aromatic
721.54	75.08	Out-of-plane deformation of aromatic rings (C-H)	Aromatic
774.05	73.39	C-H bending aliphatic	Aliphatic
808.92	71.39	Out-of-plane deformation of aromatic rings (C-H)	Aromatic
908.74	76.12	C-H aromatic bending	Aromatic
1005.29	67.85	C-O stretching	Ester
1044.43	58.81	C-O stretching	Ester
1110.44	70.53	C-O stretching alcohol	Alcohol
1164.21	56.91	C-H bending aliphatic	Aliphatic
1232.96	49.77	C-O stretching ester	Ester
1340.5	78.37	O-H deformation of phenol	Phenol
1373.73	74.45	Aromatic C-H deformation	Aromatic
1445.68	68.14	C-H bending aliphatic	Aliphatic
1486.47	80.76	C-H aromatic bending	Aromatic
1505.05	63.24	C-H bending aliphatic	Aliphatic
1583.84	83.06	C=C aromatic stretching	Aromatic
1602.23	81.01	C=C aromatic stretching	Aromatic
1711.56	67.82	C=O stretching carbonyl	Ketone/Ester/Carboxylic acid
2852.38	77.42	C-H aliphatic stretching	Aliphatic
2922.66	67.71	C-H aliphatic stretching	Aliphatic
3389.83	93.07	O-H stretching alcohol/phenol	Alcohol/Phenol

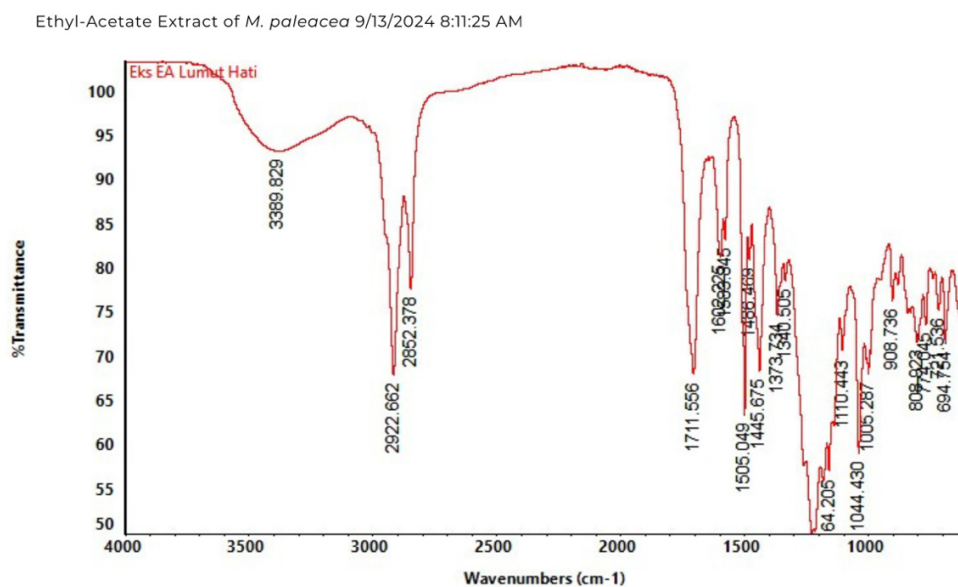


Figure 3. Fourier-transform infrared (FTIR) spectrum graph data from ethyl acetate extract of *Marchantia paleacea*. O–H (broad, ~3400 cm⁻¹): Typically corresponds to phenolic or flavonoid hydroxyl groups, which are widely recognized for antioxidant and anticancer properties; C=O (sharp, ~1700 cm⁻¹): Indicates carbonyl groups from ketones or esters, which are commonly found in cytotoxic compounds, such as terpenoids and fatty acid derivatives. C=C aromatic (~1600 cm⁻¹): Suggests the presence of aromatic rings, which are integral components of compounds such as bisbenzyls (e.g., *Marchantin* derivatives).

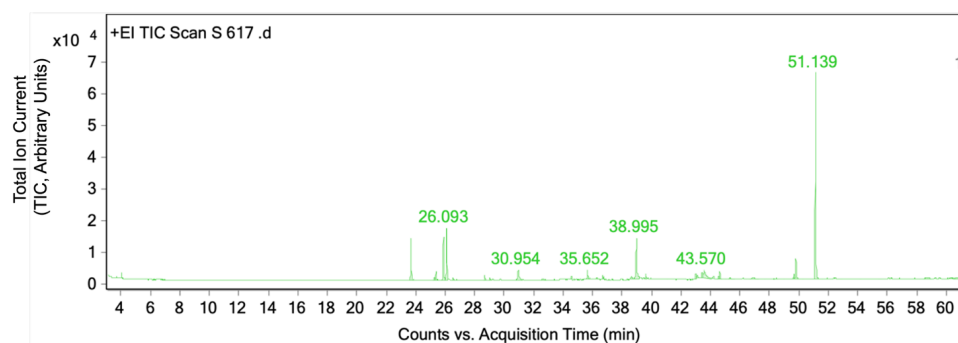


Figure 4. GC–MS chromatogram of the ethyl acetate extract of *Marchantia paleacea*. The X-axis represents the retention time (min), and the Y-axis represents the Total Ion Current (TIC, arbitrary units). The most abundant peak was detected at RT = 51.14 min (area = 250,448; 36.5%), followed by the peaks at RT = 26.09, 38.99, and 43.57 min, indicating the presence of several semi-polar constituents.

Docking validation

To ensure the reliability and reproducibility of the docking protocol, validation was performed using co-crystallized ligands retrieved from the PDB. The docking parameters, including grid box dimensions and center coordinates (x, y, z), were presented in Table 5. The co-crystallized ligands

used were STI (Imatinib) for C-Kit tyrosine kinase (PDB ID: 1T46) and QYA (5-Fluorouracil) for Cyclin-dependent kinase 2 (PDB ID: 6VJ3).

The redocking validation results were further visualized by superimposing the co-crystallized (native) and redocked ligand conformations for each protein target.

Table 3. Identified compounds, retention time (RT), peak area, and relative composition of compounds in the ethyl acetate extract of *Marchantia paleacea*, analyzed by GC-MS

No.	Compound name	Peak area	Retention time (RT)	Area %	Height
1	Phenol, 2,4-bis(1,1-dimethylethyl)-	4002.23	4.031	0.58	1604.69
2	Phytol (isomer 1)	46264.06	23.682	6.75	13245.2
3	n-Hexadecanoic acid	2904.57	25.272	0.42	806.07
4	Octadecanoic acid, methyl ester	10288.32	25.364	1.5	2841.94
5	Bis(2-ethylhexyl) phthalate	54300.74	25.877	7.92	13704.04
6	Marchantin C	60874.07	26.093	8.88	16347.38
7	Squalene	3551.54	26.534	0.52	617.54
8	Tetracosane	6203.86	28.677	0.91	1788.45
9	Phytol (isomer 2)	2677.66	29.016	0.39	716.06
10	n-Hexadecanoic acid (Palmitic acid)	20267.01	30.954	2.96	3096.31
11	Octadecanoic acid, methyl ester (Methyl stearate)	2660.87	32.605	0.39	311.64
12	9,12-Octadecadienoic acid (Linoleic acid)	3366.79	34.564	0.49	1014.9
13	Bis(2-ethylhexyl) phthalate	11668.53	35.652	1.7	2940.96
14	Squalene	3236.66	36.277	0.47	623.45
15	Phytol acetate	4203.63	36.677	0.61	1275.07
16	n-Nonadecanoic acid	2778.48	36.739	0.41	900.87
17	Neophytadiene	6435.41	38.636	0.94	1006.56
18	Marchantin C	68298.99	38.995	9.97	12642.2
19	Tetracosane	5027.79	39.611	0.73	1445.99
20	Pentacosane	7243.46	42.995	1.06	1539.33
21	Heptacosane	3867.0	43.108	0.56	702.66
22	Octacosane	8236.24	43.436	1.2	1768.53
23	Nonacosane	27589.01	43.57	4.03	2721.93
24	Phthalic acid diisooctyl ester	2913.61	44.554	0.43	919.4
25	Stigmasterol	8898.66	44.626	1.3	2509.5
26	β-Sitosterol	4179.68	45.303	0.61	414.38
27	Campesterol	6212.18	46.872	0.91	493.77
28	Cholest-5-en-3-ol (Cholesterol derivative)	2505.83	48.462	0.37	474.75
29	Lupeol	5618.33	49.662	0.82	1534.2
30	Friedelan-3-one	30205.09	49.795	4.41	6346.94
31	Marchantin A	250447.84	51.139	36.54	65343.35
32	Marchantin B	4801.45	58.749	0.7	280.87
33	Docosane	3590.5	60.811	0.52	255.2

Table 4. Lipinski rule of five (RO5) of several anti-breast cancer comparative drugs and ligand compounds from the liverwort herb of *Marchantia paleacea*

ID ligand	Lipinski rule of five				
	Mass (Da)	Hydrogen binding donor (HBD)	Hydrogen binding acceptor (HBA)	Log partition coefficient P (cLog P)	Molar refractivity (MR)
DOX	543	7	12	-0,4641	129,8884
VIO	824	3	13	3,5175	220,5687
VIB	810	3	12	3,9909	220,4288
VIC	824	3	13	3,4292	218,7888
MCA	440	3	5	6,2718	125,7263
MCB	456	4	6	5,9774	127,3911
MCC	424	2	4	6,8854	125,0056
L1	543	7	12	-0,4641	129,8884
L2	238	1	6	0,9580	56,0803
L3	308	0	2	6,3630	95,9910
L4	250	0	0	6,4910	83,7620
L5	340	0	4	5,3500	97,8100
L6	213	0	2	3,7923	61,4994
L7	196	0	2	3,2406	59,0330
L8	278	0	0	7,1677	94,0560
L9	296	1	1	6,3641	95,5618
L10	250	0	0	6,4910	83,7620
L11	208	1	1	3,6790	66,6118
L12	254	1	1	5,4820	81,8508
L13	210	1	1	4,2318	67,9758
L14	256	1	2	5,5523	77,9478
L15	144	1	1	2,7293	45,0788
L16	222	0	0	5,7108	74,5280
L17	204	0	0	4,8913	68,8330
L18	138	0	0	3,0786	43,7770
L19	168	0	0	4,5591	57,3540
L20	224	1	4	2,2644	58,5828
L21	222	1	1	3,4657	65,9968
L22	254	0	2	3,9444	59,4840
L23	204	0	0	5,2015	70,9930
L24	306	1	3	4,3496	90,4138
L25	204	0	0	4,7252	66,7430
L26	204	0	0	4,7252	66,7430
L27	204	0	0	4,7252	66,7430

DOX: Doxorubicin; VIO: Vinorelbine; VIB: Vinblastine; VIC: Vincristine; MCA: Marchantin A; MCB: Marchantin B; MCC: Marchantin C; L1: 1,2,4-Benzenetricarboxylic acid 1,2-dimethyl ester; L2: Phthalic acid di(2-propylpentyl) ester; L3: Linoleyl acetate; L4: 3-Octadec-yne; L5: Oxalic acid allyl pentadecyl ester; L6: 1-Hexyl-2-nitrocyclohexane; L7: 1,6-Octadien-3-ol, 3,7-dimethyl-, propanoate; L8: 7,11,15-trimethyl-3-hexadecene.

Table 5. Docking validation parameters of ligands 1T46 and 6VJ3 obtained from the Protein Data Bank (PDB)

PDB ID	Co-crystallized ligand	Grid Box (spacing = 0.375 Å)			Grid center coordinate		
		x	y	z	x	y	z
1T46	STI (Imatinib)	40	40	46	27.696	26.657	39.342
6VJ3	QYA (5-Fluorouracil)	40	40	40	16.567	5.451	13.121

Å: Ångström (unit of length; 1 Å: 10^{-10} m); x, y, z: Cartesian coordinates representing the center points of the docking grid box in the three-dimensional molecular space. STI: Co-crystallized ligand *Imatinib* (native ligand of PDB ID 1T46); QYA: Co-crystallized ligand *5-Fluorouracil* (native ligand of PDB ID 6VJ3).

The alignment of both poses, shown in [Figure 5](#), demonstrated a strong overlap, confirming the reliability of the docking protocol.

As detailed in [Table 5](#), the docking grids were set to encompass all ligands, with parameters validated by the Lamarckian genetic algorithm (100 GA runs, medium evals). Ligand overlays ([Figure 5](#)) showed RMSD values ≤

2 Å, confirming docking accuracy.

Docking ligand

The ligands were optimized and docked to each target using the Lamarckian genetic algorithm. For 1T46 ([Table 6](#)). Marchantin C (MCC) showed the lowest binding energy (−8.62 kcal/mol), indicating the highest affinity, followed

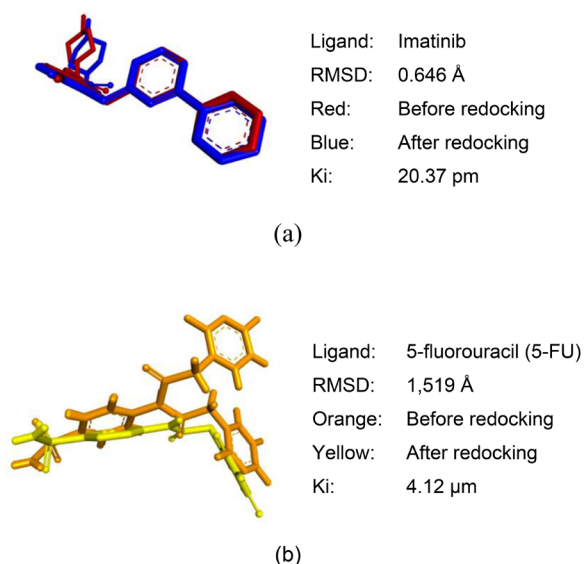


Figure 5. Overlay of imatinib ligand co-crystals on the 1T46 target (a) and co-crystal overlay of 5-fluorouracil (5-FU) ligand on 6VJ3 target (b).

by Marchantin A (−8.14 kcal/mol) and B (−7.96 kcal/mol). Doxorubicin (−6.99 kcal/mol) and the comparators had higher energies, with key interacting residues identified for each ligand. Other ligands showed lower affinities but may still be of interest for further study.

The active site interactions for 1T46 involved residues D810, E640, V643, and F811 (Table 6). Marchantin C, stigmaterol, and Marchantin B showed strong binding (−8.62 to −6.79 kcal/mol). In contrast, ligands 7 and 11 exhibited positive binding energies (+0.24 to +0.87 kcal/

mol) in 3POZ, indicating unfavorable interactions, and were therefore excluded from further analysis.

Marchantin C (MCC) exhibited the highest binding affinity to 6VJ3 (−8.62 kcal/mol), followed by Marchantin A and B (−8.14 and −7.96 kcal/mol, respectively). Key residues included P202, N62, T199, and V135. Doxorubicin and COZ displayed lower affinities (−6.99 and −7.35 kcal/mol). Other compounds, such as L2 and L5, exhibited even weaker binding (Table 7). These results highlight MCC as a promising candidate for further exploration as a natural therapeutic agent for 6VJ3.

Discussion

The three liquid extracts were evaporated under controlled temperature and pressure to obtain concentrated samples for further analysis (16). FTIR and GC-MS analyses consistently identified key bioactive compounds (Marchantin A, B, and C) containing functional groups, such as phenolic O–H, aromatic rings, and carbonyls. These groups are closely linked to antioxidant and anticancer activities, supporting the observed cytotoxic effects in MCF-7 and T47D cells (17).

The EAEMP demonstrated the highest cytotoxic and anticancer activity among all fractions, which can be attributed to the presence of semi-polar bioactive constituents, including flavonoids, phenols, bisbibenzyls, and terpenoids, that are widely reported for their anticancer mechanisms (18). The n-hexane extract exhibited weaker effects, indicating that the most active compounds in *M. paleacea* are more soluble in semi-polar or polar solvents

Table 6. Docking results of various ligands to target 1T46 using the Lamarckian genetic algorithm method

No.	Ligand code	Compound interactions (Amino acid compound residues/Active site) of target 1T46		Docking results	
		Hydrogen bonds	Hydrophobic interactions	Binding energy (kcal/mol)	Inhibition constant (μm)
1	COZ	C673, D810, H290	K623, T670, L644, L799, L595	−12.64	0.00002037
2	DOX	T670, E640, C788, H790, I808, A636	V668, K623, L644, V643, C788	−5.74	62.17
3	VIO	L647, C809, E640	V654, L813, L637, K623, R791, V643	+50.66	n/a
4	VIB	R791, E640, C728	V654, C809, L647	+23.52	n/a
5	VIC	I808, L783, E640	V643, R791, V654	+53.22	n/a
6	MCA	R791, D810, H790, L644, I808, V654	E640, C788, I653, L783, V643	−5.78	58.25
7	MCB	–	D810, H790, C788, L783, C809, I653, I808, E640, L644, V643	−4.23	791.82
8	MCC	D810, C809	E640, L644, L783, V643, I808, I653, C788	−7.7	2.28
9	L1	C763, Y672, L595, T670, L623, D810	A621, V603, L799	−6.57	15.37
10	L2	L623, D810, E640	V668, T670, L644, V643, I653, L783, I808, A621, Y672, C673, F811, L595, L799, V603, C809	−9.94	0.05148
11	L3	Y672, C672, T670, E640, D810	L595, F811, L799, A621, V603, L623, V654, L644, V668, C809, I653, I808	−7.71	2.24
12	L4	–	C673, V654, C809, V603, L644, K623, V668, L799, A621, Y672, L595	−6.81	10.18
13	L5	Y672, C673	L644, K623, C809, V654, F811, V603, A621, L799, L595	−6.88	9.13

Table 6. Continued

No.	Ligand code	Compound interactions (Amino acid compound residues/Active site) of target 1T46		Docking results	
		Hydrogen bonds	Hydrophobic interactions	Binding energy (kcal/mol)	Inhibition constant (μm)
14	L6	D810, K623, L644	C809, L799, F811, V654, V603, V668, A621	-8.1	1.15
15	L7	K623, L799, D810, E640	A621, F811, V668, V603, C809, V654, L644	-6.9	8.76
16	L8	D810, K623, E640	L783, H790, I653, I808, L644, C809, A621, V603, L799, F811, L595, C673	-7.91	1.60
17	L9	T670, L644	Y672, C673, L595, L799, A621, V603, C809, F811, K623, V654	-8.21	0.96107
18	L10	T670	K623, L644, V668, V654, V603, C809, A621, F811, L595, L799, C672, Y672	-6.75	11.23
19	L11	C673, E671, Y672, L644, V668	V654, K623, L799, F811, C809, V603, A621	-5.88	48.70
20	L12	D810, E640, C809, F811	V668, L644, A621, Y672, C673, L595, L799, V603, V654	-6.88	9.07
21	L13	V668, E640, D810, C673, Y672, L644	K623, F811, V603, C809, A621, V654, L799, L595	-6.32	23.48
22	L14	C673	L799, F811, L595, V603, C809, V654, A621, K623, C668	-6.43	19.21
23	L15	V668, E640, D810	K623, A621, V603, F811, L799, V654, C809	-4.64	400.07
24	L16	D810	F811, C809, V654, K623, V603, L595, L799, C673, A621, Y672	-6.51	17.05
25	L17	L799, L595	K623, A621, V603, V654, C809, F811	-7.74	2.14
26	L18	F811, K623, A621, V603	V654, L644, C809	-5.17	161.09
27	L19	L644	V668	-5.5	92.34
28	L20	D810, T670	V668	-7.53	3.04
29	L21	T670	-	-7.43	3.56
30	L22	T670, V622, G676	V668	-5.82	54.47
31	L23	-	A621, V603, C668, K623, L644, C809, V654, I653, H790, I808	-7.23	5.01
32	L24	E640, L644, K623	V654, L799, A621, V603, L595, C809	-7.98	1.40
33	L25	E640, L595	V668, K623, V654, V603, C809, C673, A621, L799	-8.13	1.09
34	L26	K623, C673	V654, C809, V603, L595, Y672, L799, A621	-8.01	1.35
35	L27	V654, C809, L799, F811	V603, K623, A621	-7.6	2.69

COZ: Co-crystallized ligand; DOX: Doxorubicine (i.v.); VIO: Vinorelbine (i.v.); VIB: Vinblastine (i.v.); VIC: Vincristine (i.v.); MCA: Marchantin A; MCB: Marchantin B; MCC: Marchantin C; L1: 1,2,4-Benzenetricarboxylic acid,1,2-dimethyl ester; L2: Phthalic acid, di(2-propylpentyl) ester; L3: Linoleyl acetate; L4: 3-Octadecyne; L5: Oxalic acid, allyl pentadecyl ester; L6: 1-Hexyl-2-nitrocyclohexane; L7: 1,6-Octadien-3-ol, 3,7-dimethyl-, propanoate; L8: 7,11,15-trimethyl-3-methylidenehexadec-1-ene; L9: Phytol; L10: 1-Octadecyne; L11: tetradec-13-en-11-yn-1-ol; L12: (R)-(Z)-14-Methyl-8-hexadecen-1-ol; L13: E-11,13-Tetradecadien-1-ol; L14: n-Hexadecanoic acid; L15: 1-Nonanol; L16: 1-Hexadecyne; L17: 1-Cycloheptene, 1,4-dimethyl-3-(2-methyl-1-propene-1-yl)-4-vinyl-; L18: 1,1'-Bicyclopropyl, 2,2,2',2'-tetramethyl-; L19: 1-Undecene, 9-methyl-; L20: 4-Hydroxy-6-methyl-3-(4-methylpentanoyl)-2H-pyran-2-one; L21: (1aR,4R,4aR,7S,7aS,7bS)-1,1,4,7-tetramethyldecahydro-1H-cyclopropa[e]azulen-4-ol; L22: Acetic acid, trifluoro-, 3,7-dimethyloctyl ester; L23: (3E,6E)-3,7,11-trimethyldodeca-1,3,6,10-tetraene; L24: 2,4-di-tert-butylphenyl 5-hydroxypentanoate; L25: Phytol; L26: Hexadecanoic acid, methyl ester (methyl palmitate); L27: 9,12-Octadecadienoic acid (Z,Z)-, methyl ester (methyl linoleate).

(19). Although the EEMP showed the lowest cytotoxicity, it may still have potential applications that require lower levels of cytotoxic activity (20).

The efficacy of doxorubicin was much stronger than that of all the extracts, which is in accordance with its role as a proven anticancer agent (21). These compounds are known to induce apoptosis (such as S and G2/M) by regulating the expression of apoptosis-related proteins, such as BAX, BCL-2, caspase, and p53, inhibit proliferation, and modulate key molecular pathways, as supported by studies on other ethyl acetate plant extracts (22). Normalized absorbance (%) enables consistent comparison of cytotoxicity results across different

concentrations and conditions (23).

Marchantia paleacea is a traditional medicinal plant rich in macrocyclic bisbibenzyls, such as marchantin A and C, which are unique to liverworts. These compounds exhibit diverse pharmacological activities, including antimicrobial, anti-inflammatory, antioxidant, and potential anticancer effects (24). Marchantin A exhibits strong anticancer activity by inducing apoptosis and regulating genes involved in the cell cycle and apoptosis pathways in cancer cells (25). In addition, Marchantin C and E have been shown to exert cytotoxic effects on several cancer cell types (26-28). Ethyl acetate extracts from various plants, such as *Cordyceps sinensis*, *Peltophorum*

Table 7. Docking results of various ligands to the 6VJ3 target using the Lamarckian genetic algorithm method

No	Ligand code	Compound interactions (Amino acid compound residues/Active site) of target 6VJ3		Docking result	
		Hydrogen bonds	Hydrophobic interactions	Binding energy (kcal/mol)	Inhibition constant (μm)
1	COZ	H94, H119, H96, T199, T200	I91, Q92, V121, L198	7.35	4.12
2	DOX	N62, Q92, N67, T200, T199, H96, H119, V121	V135, P202, F131, L204, L198, W209, V143	-6.99	7.53
3	VIO	I91, L198, P202, P201, Q92, W5, N62, H64, N67, T200	H94, A65	-5.11	181.07
4	VIB	V135, P202, P201, L198, N62, H94, N67	F131	-6.72	11.88
5	VIC	F131, P201, N67, Q92, N62, H64, W5	V135, L198, P202	-6.12	32.67
6	MCA	V143, L198, V121, N67, H94, H119	F131, T200	-8.14	1.07
7	MCB	N62, N67, F131, H119, T199, T200	L198	-7.96	1.46
8	MCC	P202, N62, N67, T199	V135, L198, A65, H94	-8.62	0.48225
9	L1	W209, H94, H96, H119, Y7, T200, N62, N67, T199	-	-5.87	49.58
10	L2	H96, P201, H119, T199, N62, Q92, H94, N67	T200, A65, P202, W209, V207, L198, V143, V121	-6.33	22.88
11	L3	T200, P202, F131, Q92, T199	H119, W209, V143, L198, A65, V121, H94	-5.62	75.46
12	L4	T199, T200	H94, H64, A65, H96, H119, V143, V121, V207, L198, P202	-4.72	349.62
13	L5	V207, W209, H118, H96, T199, H94, P202	V143, L141, V121, L198, H64, W5, A65	-5.40	109.17
14	L6	H1H94, H96, T199, H64, W5, L141	V121, L198, V143, A65	-6.35	22.17
15	L7	H119, H94, H96, V143, T199	A65, H64, L198	-5.91	46.78
16	L8	L198, T199	W209, V143, H119, A65, W5, H64, H96, H94	-5.64	73.09
17	L9	H64, W5, H94, H119, H96, V143, W209	A65, L198, V121	-6.00	39.98
18	L10	-	A65, H96, H94, V143, V121, F131, L198, H119, P202, V135	-4.67	378.34
19	L11	H119, H94, H96	V207, V143, W209, L198, V121, A65	-4.92	245.45
20	L12	H94, H96	A65, V121, L198, W209, H119, V143	-5.28	135.28
21	L13	H94, H119	A65, H96, V121, V143, L198, W209	-4.95	235.89
22	L14	H95, H96, W209, H119, T199	A65, V143, L198, V121	-4.98	223.09
23	L15	H94, H119, H96, T199	V121, L198, V143	-4.25	763.78
24	L16	-	V143, V121, W209, H96, H119, A65, H94, L198	-4.61	415.65
25	L17	H96, H94, H119	F131, V121, L198, V143, V207, W209	-6.23	27.30
26	L18	V207, V121, V143, W209, L198	-	-5.08	187.72
27	L19	-	A65, H94, H96, V207, H119, V143, W209, L198	-4.54	467.73
28	L20	H94, H119, Q92	V207, 209, V143, V121, L198, H96, A165	-6.51	16.84
29	L21	Q92, H96, H94, H119, W209	F131, V121, L198	-7.01	7.33
30	L22	T199, V121, H96, H94, H119, T200, F131	A65, L198	-5.47	98.40
31	L23	A65, T200, H96, T199	H64, W5, H94, W209, H119, V143, L198, V207	-5.73	63.35
32	L24	H64, W5, Q92, V207, N62, N67	H94, V143, L198, H119, W209	-7.09	6.37
33	L25	Q92, N62, N67, H119, W209	V121, F131, V143, V297, L198, H94	-7.00	7.34
34	L26	-	V121, L198, V143, H94	-6.47	18.00
35	L27	-	V121, H94, L198, V143	-6.97	7.80

COZ: Co-crystalized Ligand; DOX: Doxorubicine (i.v.); VIO: Vinorelbine (i.v.); VIB: Vinblastine (i.v.); VIC: Vincristine (i.v.); MCA: Marchantin A; MCB: Marchantin B; MCC: Marchantin C; L1: 1,2,4-Benzenetricarboxylic acid,1,2-dimethyl ester; L2: Phthalic acid, di(2-propylpentyl) ester; L3: Linoleyl acetate; L4: 3-Octadecyne; L5: Oxalic acid, allyl pentadecyl ester; L6: 1-Hexyl-2-nitrocyclohexane; L7: 1,6-Octadien-3-ol, 3,7-dimethyl-, propanoate; L8: 7,11,15-trimethyl-3-methylidenehexadec-1-ene; L9: Phytol; L10: 1-Octadecyne; L11: tetradec-13-en-11-yn-1-ol; L12: (R)-(Z)-14-Methyl-8-hexadecen-1-ol; L13: E-11,13-Tetradecadien-1-ol; L14: n-Hexadecanoic acid; L15: 1-Nonanol; L16: 1-Hexadecyne; L17: 1-Cycloheptene, 1,4-dimethyl-3-(2-methyl-1-propene-1-yl)-4-vinyl-; L18: 1,1'-Bicyclopropyl, 2,2,2',2'-tetramethyl-; L19: 1-Undecene, 9-methyl-; L20: 4-Hydroxy-6-methyl-3-(4-methylpentanoyl)-2H-pyran-2-one; L21: (1aR,4R,4aR,7S,7aS,7bS)-1,1,4,7-tetramethyldecahydro-1H-cyclopropa[e]azulen-4-ol; L22: Acetic acid, trifluoro-, 3,7-dimethyloctyl ester; L23: (3E,6E)-3,7,11-trimethyldodeca-1,3,6,10-tetraene; L24: 2,4-di-tert-butylphenyl 5-hydroxypentanoate; L25: Phytol; L26: Hexadecanoic acid, methyl ester (methyl palmitate); L27: 9,12-Octadecadienoic acid (Z,Z)-, methyl ester (methyl linoleate).

africanum, and *Clitoria ternatea*, significantly inhibited the proliferation of MCF-7 cancer cells, with low IC₅₀ values, indicating their potential as strong anticancer agents (29).

Spectral data confirmed the presence of functional groups, such as phenols and carbonyls, which may underlie the biological activity of the extract (30). The presence of hydroxyl (O-H), carbonyl (C=O), and aromatic C=C groups indicates the presence of phenolic or flavonoid compounds, which are known to exhibit antioxidant and cytotoxic activities (31). Compounds such as phenols and carbonyls are prime candidates for supporting cytotoxic activity against cancer cells (e.g., such as MCF-7 and T47D cells) (32).

Macrocyclic bis(bibenzyl)s are unique phytochemicals found only in liverworts (33). Semi-polar solvents, such as ethyl acetate, effectively extract macrocyclic bis(bibenzyl)s from *M. paleacea*, which exhibit notable cytotoxic and antimicrobial activities (34). Marchantin A, B, and C have high biological potency but exceed Lipinski's log P threshold, indicating poor oral absorption and greater suitability for non-oral use. Standard drugs, such as doxorubicin and vinblastine analogs, violate Lipinski's criteria because of their high molecular weights (35). Standard compounds, such as doxorubicin and vinblastine, are effective in intravenous formulations but have limitations in oral applications (36). According to Lipinski's rule, compounds with a molecular weight >500 Da or log P > 5 may have poor absorption and bioavailability (37,38).

Optimization was performed using the Gaussian quantum method, with the Density Functional Theory Basis Set 6-31G and the B3LYP function (39). An optimization method was employed to determine the coordinates that minimized the energy in the system, thereby obtaining the geometric structure of the molecule (40). After the limits were adjusted, the docking parameter addition process was performed using the Lamarckian genetic algorithm method with 100 GA Runs (41). The docking method was validated by accurately separating and redocking the co-crystallized ligands into the active site using unchanged grid parameters and protocols (42). Only ligands with RMSD ≤ 2 Å and negative binding energies were considered for further biological interpretation, aligning the docking results with the observed cytotoxicity (43).

The structures of key bioactive compounds, such as Marchantin C and stigmasterol, influenced their strong docking affinities and cytotoxic effects, highlighting the importance of molecular structure in predicting anticancer activity (44). The literature consistently demonstrates that bisbibenzyls from *Marchantia* species, such as Marchantin A, exhibit notable anticancer activity against breast cancer cell lines (5). Recent studies have confirmed that Marchantin A and C induce apoptosis and cell cycle arrest

in breast cancer cells, supporting our findings that link their structures to strong anticancer activities (45).

While molecular docking provides preliminary insights into ligand-protein interactions, future studies using molecular dynamics simulations and MM-PBSA analyses are needed for a deeper validation of binding stability and affinity (46). The key residues identified in the 1T46 target active site (D810, E640, V643, and F811) were consistent with those of prior docking studies, supporting the reliability of our predictions (44).

This study had several limitations that should be acknowledged. The cytotoxic evaluation was limited to in vitro assays using two breast cancer cell lines (MCF-7 and T47D); therefore, it may not fully represent the complex interactions occurring in vivo. Additionally, the *in silico* analysis was based on predicted binding affinities and molecular docking simulations, which require further biochemical and pharmacokinetic validation. Future studies should include in vivo investigations to confirm the anticancer efficacy and safety of *M. paleacea* extracts, as well as advanced molecular assays to elucidate the underlying mechanisms of apoptosis and cell cycle regulation. Moreover, isolation and structural characterization of the active constituents, followed by target-specific binding assays, would provide deeper insights into their therapeutic potential as natural anticancer agents.

Conclusion

This study demonstrated that the EAEMP exhibits significant cytotoxic activity against breast cancer cell lines MCF-7 and T47D, with IC₅₀ values of 8.681 µg/mL and 12.78 µg/mL, respectively. GC-MS profiling identified bioactive constituents, notably Marchantin C, which exhibited a strong binding affinity with key anticancer targets in docking simulations (−8.62 kcal/mol with the protein kinase domain). This compound also established stable hydrogen bonding with the active site residues D810 and E640. These findings highlight the therapeutic potential of *M. paleacea* as a source of natural cytotoxic agents, specifically through its phenolic and bisbibenzyl components.

Acknowledgements

The authors would like to express their sincere gratitude to the research team and staff at the Pharmacy Department, Poltekkes Kemenkes Bandung, for their assistance in the extraction and preliminary phytochemical analysis of *M. paleacea*. Appreciation is also extended to the Central Laboratory of Padjadjaran University for providing access to GC-MS and FTIR instrumentation, and to the Cell Culture and Cytogenetics Laboratory, Faculty of Medicine, Universitas Padjadjaran, for supporting the cytotoxicity assays on MCF-7 and T47D breast cancer cell lines. The authors are also grateful to Prof. Ahmad Faried,

Dr., Sp.BS(K), Ph.D., for kindly providing the MCF-7 cell line, and Dr. Med. M. Hasan Bashari, Dr. M.Kes., for facilitating access to the T47D cell line used in this study.

Authors' contribution

Conceptualization: Dicki Bakhtiar Purkon, Faizah Min Fadhlillah, Irvan Herdiana.

Data curation: Dicki Bakhtiar Purkon, Muhamad Iqbal Rhamadiano, Jihan Amirah Salsabila, Putri Dwi Handayani.

Formal analysis: Dicki Bakhtiar Purkon, Muhamad Iqbal Rhamadiano, Eva Dania Kosasih, Nur Aji.

Investigation: Dicki Bakhtiar Purkon, Muhamad Iqbal Rhamadiano, Irvan Herdiana, Jihan Amirah Salsabila, Putri Dwi Handayani.

Methodology: Dicki Bakhtiar Purkon, Irvan Herdiana, Muhamad Iqbal Rhamadiano, Faizah Min Fadhlillah.

Resources: Dicki Bakhtiar Purkon, Muhamad Iqbal Rhamadiano, Faizah Min Fadhlillah.

Validation: Mimin Kusmiyati, Irvan Herdiana, Nur Aji, Eva Dania Kosasih.

Visualization: Dicki Bakhtiar Purkon, Irvan Herdiana, Muhamad Iqbal Rhamadiano, Faizah Min Fadhlillah.

Writing-original draft: Dicki Bakhtiar Purkon.

Writing-review & editing: Mimin Kusmiyati, Irvan Herdiana, Nur Aji, Eva Dania Kosasih, Faizah Min Fadhlillah, Dicki Bakhtiar Purkon.

Conflict of interests

The authors declared no conflict of interest in this manuscript.

Funding/Support

This research was funded by the Competitive Decentralization Research Grants from the Directorate General of Health Workers, Ministry of Health, Republic of Indonesia, under contract number DP.04.03/F. XVIII/930/2024.

References

- Kinnel B, Singh SK, Oprea-Ilie G, Singh R. Targeted therapy and mechanisms of drug resistance in breast cancer. *Cancers (Basel)*. 2023;15(4):1320. doi: 10.3390/cancers15041320.
- Siregar ES, Pasaribu N, Sofyan MZ. Antioxidant activity of liverworts *Marchantia paleacea* Bertol. from North Sumatra Indonesia. *IOP Conf Ser Earth Environ Sci*. 2021;713(1):012061. doi:10.1088/1755-1315/713/1/012061.
- Liu N, Wang SQ, Lou HX. Chemical constituents of *Marchantia paleacea*. *Chem Nat Compd*. 2018;54(3):541-4. doi: 10.1007/s10600-018-2400-5.
- Asakawa Y, Ludwiczuk A, Novakovic M, Bukvicki D, Anchang KY. Bis-bibenzyls, bibenzyls, and terpenoids in 33 genera of the Marchantiophyta (liverworts): structures, synthesis, and bioactivity. *J Nat Prod*. 2022;85(3):729-62. doi: 10.1021/acs.jnatprod.1c00302.
- Jensen JS, Omarsdottir S, Thorsteinsdottir JB, Ogmundsdottir HM, Olafsdottir ES. Synergistic cytotoxic effect of the microtubule inhibitor marchantin A from *Marchantia polymorpha* and the Aurora kinase inhibitor MLN8237 on breast cancer cells in vitro. *Planta Med*. 2012;78(5):448-54. doi: 10.1055/s-0031-1298230.
- Jabir NR, Rehman MT, AlAjmi MF, Ahmed BA, Tabrez S. Prioritization of bioactive compounds envisaging yohimbine as a multi targeted anticancer agent: insight from molecular docking and molecular dynamics simulation. *J Biomol Struct Dyn*. 2023;41(20):10463-77. doi: 10.1080/07391102.2022.2158137.
- Wakeel A, Jan SA, Ullah I, Shinwari ZK, Xu M. Solvent polarity mediates phytochemical yield and antioxidant capacity of *Isatis tinctoria*. *PeerJ*. 2019;7:e7857. doi: 10.7717/peerj.7857.
- Yu S, Kim T, Yoo KH, Kang K. The T47D cell line is an ideal experimental model to elucidate the progesterone-specific effects of a luminal A subtype of breast cancer. *Biochem Biophys Res Commun*. 2017;486(3):752-8. doi: 10.1016/j.bbrc.2017.03.114.
- Benov L. Improved formazan dissolution for bacterial MTT assay. *Microbiol Spectr*. 2021;9(3):e0163721. doi: 10.1128/spectrum.01637-21.
- Hefny Gad M, Tuentner E, El-Sawi N, Younes S, El-Ghadban EM, Demeyer K, et al. Identification of some bioactive metabolites in a fractionated methanol extract from *Ipomoea aquatica* (aerial parts) through TLC, HPLC, UPLC-ESI-QTOF-MS and LC-SPE-NMR fingerprints analyses. *Phytochem Anal*. 2018;29(1):5-15. doi: 10.1002/pca.2709.
- Ji W, Wallace WE. Comprehensive data evaluation methods used in developing the SWGDRUG mass spectral reference library for seized drug identification. *Anal Chem*. 2024;96(42):17004-12. doi: 10.1021/acs.analchem.4c04425.
- Wu YF, Zheng HB, Liu XY, Cheng AX, Lou HX. Molecular diversity of alkenal double bond reductases in the liverwort *Marchantia paleacea*. *Molecules*. 2018;23(7). doi: 10.3390/molecules23071630.
- Nguyen NT, Nguyen TH, Pham TN, Huy NT, Bay MV, Pham MQ, et al. Autodock Vina adopts more accurate binding poses but Autodock4 forms better binding affinity. *J Chem Inf Model*. 2020;60(1):204-11. doi: 10.1021/acs.jcim.9b00778.
- Rizvi SM, Shakil S, Haneef M. A simple click by click protocol to perform docking: AutoDock 4.2 made easy for non-bioinformaticians. *EXCLI J*. 2013;12:831-57.
- Gurung R, Yirsaw AW, Khodary MG, Samuel T, Sandey M, Yates CC, et al. Abstract 5945: exploring the antiproliferative potential of KHS101 on triple negative breast cancer cell lines. *Cancer Res*. 2024;84(6 Suppl):5945. doi: 10.1158/1538-7445.am2024-5945.
- Osik NA, Lukzen NN, Yanshole VV, Tsentalovich YP. Loss of volatile metabolites during concentration of metabolomic extracts. *ACS Omega*. 2024;9(22):24015-24. doi: 10.1021/acsomega.4c02439.
- Pezhhanfar S, Farajzadeh MA, Hosseini-Yazdi SA, Afshar Mogaddam MR. NiGA MOF-based dispersive micro solid phase extraction coupled to temperature-assisted evaporation using low boiling point solvents for the extraction and preconcentration of butylated

- hydroxytoluene and some phthalate and adipate esters. RSC Adv. 2023;13(43):30378-90. doi: 10.1039/d3ra04612e.
18. Abou Baker DH. *Achillea millefolium* L. ethyl acetate fraction induces apoptosis and cell cycle arrest in human cervical cancer (HeLa) cells. Ann Agric Sci. 2020;65(1):42-8. doi: 10.1016/j.aos.2020.03.003.
 19. Tabakam GT, Kodama T, Tchuemogne MA, Hoang NN, Nomin-Erdene B, Ngouela SA, et al. Cytotoxic potential of dihydrochalcones from *Eriosema glomeratum* and their semi-synthetic derivatives. Nat Prod Res. 2024;38(2):186-97. doi: 10.1080/14786419.2022.2111563.
 20. Lee CS, Kim TW, Oh DE, Bae SO, Ryu J, Kong H, et al. In vivo and in vitro anticancer activity of doxorubicin-loaded DNA-AuNP nanocarrier for the ovarian cancer treatment. Cancers (Basel). 2020;12(3):634. doi: 10.3390/cancers12030634.
 21. Buranrat B, Sangdee K, Sangdee A. Comparative study on the effect of aqueous and ethanolic mycelial extracts from *Polycephalomyces nipponicus* (Ascomycetes) against human breast cancer MCF-7 cells. Int J Med Mushrooms. 2019;21(7):671-81. doi: 10.1615/IntJMedMushrooms.2019031140.
 22. Lem FF, Cheong BE, Teoh PL. *Ruellia tuberosa* ethyl acetate leaf extract induces apoptosis and cell cycle arrest in human breast cancer cell line, MCF-7. Sci Pharm. 2022;90(3):44. doi: 10.3390/scipharm90030044.
 23. Zaharieva L, Stoyanova M, Dimova V, Genova TS, Antonov L, Markovski A, et al. Absorbance measurement for interdisciplinary educational experiment on cytotoxicity. Phys Educ. 2024;59(6):065018. doi: 10.1088/1361-6552/ad7a45.
 24. Liu N, Wang SQ, Lou HX. Chemical constituents of *Marchantia paleacea*. Chem Nat Compd. 2018;54(3):541-4. doi: 10.1007/s10600-018-2400-5.
 25. Huang WJ, Wu CL, Lin CW, Chi LL, Chen PY, Chiu CJ, et al. Marchantin A, a cyclic bis(bibenzyl ether), isolated from the liverwort *Marchantia emarginata* subsp. *tosana* induces apoptosis in human MCF-7 breast cancer cells. Cancer Lett. 2010;291(1):108-19. doi: 10.1016/j.canlet.2009.10.006.
 26. Shi YQ, Zhu CJ, Yuan HQ, Li BQ, Gao J, Qu XJ, et al. Marchantin C, a novel microtubule inhibitor from liverwort with anti-tumor activity both in vivo and in vitro. Cancer Lett. 2009;276(2):160-70. doi: 10.1016/j.canlet.2008.11.004.
 27. Jiang J, Sun B, Wang YY, Cui M, Zhang L, Cui CZ, et al. Synthesis of macrocyclic bisbibenzyl derivatives and their anticancer effects as anti-tubulin agents. Bioorg Med Chem. 2012;20(7):2382-91. doi: 10.1016/j.bmc.2012.02.004.
 28. Xu AH, Hu ZM, Qu JB, Liu SM, Syed AK, Yuan HQ, et al. Cyclic bisbibenzyls induce growth arrest and apoptosis of human prostate cancer PC3 cells. Acta Pharmacol Sin. 2010;31(5):609-15. doi: 10.1038/aps.2010.37.
 29. Rollando R, Amelia MA, Afthoni MH, Prilianti KR. Potential cytotoxic activity of methanol extract, ethyl acetate, and n-hexane fraction from *Clitoria ternatea* L. on MCF-7 breast cancer cell line and molecular docking study to P53. J Pure Appl Chem Res. 2023;12(1):7-14. doi: 10.21776/ub.jpacr.2023.012.01.705.
 30. Dabulici CM, Sârbu I, Vamanu E. The bioactive potential of functional products and bioavailability of phenolic compounds. Foods. 2020;9(7):953. doi: 10.3390/foods9070953.
 31. Rao YK, Geethangili M, Fang SH, Tzeng YM. Antioxidant and cytotoxic activities of naturally occurring phenolic and related compounds: a comparative study. Food Chem Toxicol. 2007;45(9):1770-6. doi: 10.1016/j.fct.2007.03.012.
 32. Lu HY, Zhu JS, Xie J, Zhang Z, Zhu J, Jiang S, et al. Hydroxytyrosol and oleuropein inhibit migration and invasion via induction of autophagy in ER-positive breast cancer cell lines (MCF7 and T47D). Nutr Cancer. 2021;73(2):350-60. doi: 10.1080/01635581.2020.1750661.
 33. Esumi T, Wada M, Mizushima E, Sato N, Kodama M, Asakawa Y, et al. Efficient synthesis of isoplagiochin D, a macrocyclic bis(bibenzyls), by utilizing an intramolecular Suzuki-Miyaura reaction. Tetrahedron Lett. 2004;45(37):6941-5. doi: 10.1016/j.tetlet.2004.07.068.
 34. Ivković I, Novaković M, Veljić M, Mojsin M, Stevanović M, Marin PD, et al. Bis-bibenzyls from the liverwort *Pellia endiviifolia* and their biological activity. Plants (Basel). 2021;10(6):1063. doi: 10.3390/plants10061063.
 35. Lohit N, Singh AK, Kumar A, Singh H, Yadav JP, Singh K, et al. Description and *in silico* ADME studies of US-FDA approved drugs or drugs under clinical trial which violate the Lipinski's rule of 5. Lett Drug Des Discov. 2024;21(8):1334-58. doi: 10.2174/1570180820666230224112505.
 36. Lee J, Choi MK, Song IS. Recent advances in doxorubicin formulation to enhance pharmacokinetics and tumor targeting. Pharmaceuticals (Basel). 2023;16(6):802. doi: 10.3390/ph16060802.
 37. Cui Y, Desevaux C, Truebenbach I, Sieger P, Klinder K, Long A, et al. A bidirectional permeability assay for beyond rule of 5 compounds. Pharmaceutics. 2021;13(8):1146. doi: 10.3390/pharmaceutics13081146.
 38. Ivanović V, Rančić M, Arsić B, Pavlović A. Lipinski's rule of five, famous extensions and famous exceptions. Chemia Naissensis. 2020;3(1):171-81. doi: 10.46793/ChemN3.1.171I.
 39. Muzomwe M, Maes G, Kasende OE. Theoretical DFT(B3LYP)/6-31+G(d) study on the prediction of the preferred interaction site of 3-methyl-4-pyrimidone with different proton donors. Nat Sci (Irvine). 2012;4(5):286-97. doi: 10.4236/ns.2012.45041.
 40. Karakaş Sarıkaya E, Dereli Ö, Bahçeli S. A comparative study of DFT/B3LYP/6-31G(d,p), RM062X/6-31G(d,p), B3LYP/6-311++G(d,p) and HSEH1PBE/6-31G(d,p) methods applied to molecular geometry and electronic properties of Cs-C60Cl6 molecule. Adiyaman Univ J Sci. 2021;11(2):456-73. doi: 10.37094/adyujsci.938050.
 41. Ross BJ. A Lamarckian Evolution Strategy for Genetic Algorithms. CRC Press; 2019. doi: 10.1201/9780429128356-1.
 42. Bhojwani HR, Joshi UJ. Pharmacophore and docking guided virtual screening study for discovery of type I inhibitors of VEGFR-2 kinase. Curr Comput Aided Drug Des. 2017;13(3):186-207. doi: 10.2174/1386207319666161214112536.
 43. Muttaqin FZ, Ismail H, Muhammad HN. Studi molecular docking, molecular dynamic, dan prediksi toksisitas senyawa turunan alkaloid naftiridin sebagai inhibitor protein kasein kinase 2- α pada kanker leukemia. Pharmacoscript.

- 2019;2(2):131-51. doi: 10.36423/pharmacoscript.v2i2.241.
44. Hobbs HT, Shah NH, Badroos JM, Gee CL, Marqusee S, Kuriyan J. Differences in the dynamics of the tandem-SH2 modules of the Syk and ZAP-70 tyrosine kinases. *bioRxiv* [Preprint]. July 21, 2021. Available from: <https://www.biorxiv.org/content/10.1101/2021.07.20.453126v2>.
 45. Sen K, Khan MI, Paul R, Ghoshal U, Asakawa Y. Recent advances in the phytochemistry of bryophytes: distribution, structures and biological activity of bibenzyl and bisbibenzyl compounds. *Plants (Basel)*. 2023;12(24):4173. doi: 10.3390/plants12244173.
 46. Fuhrmann J, Rurainski A, Lenhof HP, Neumann D. A new Lamarckian genetic algorithm for flexible ligand-receptor docking. *J Comput Chem*. 2010;31(9):1911-8. doi: 10.1002/jcc.21478.

Copyright © 2026 The Author(s). This is an open-access article distributed under the terms of the Creative Commons Attribution License (<http://creativecommons.org/licenses/by/4.0>), which permits unrestricted use, distribution, and reproduction in any medium, provided the original work is properly cited.